4th Flow Control Conference
23 - 26 June 2008, Seattle, Washington

AIAA 2008-4078

The Utility of Hysteresis for Closed-Loop Control Applications that Maintain Attached Flow under Natural Post Stall Conditions on Airfoils

Boris Zakharin*, Philipp Tewes†, Chunmei Chen‡ and Israel J. Wygnanski§
The University of Arizona, Tucson, AZ, 85721

and

Anthony E. Washburn**
NASA Langley Research Center

Much higher control input is required to attach separated flow than to keep an attached flow from separating under natural, post stall conditions. The experiments with slot suction applied near the leading-edge, revealed a hysteresis of lift and drag coefficients that depend on the level of suction. This offers an opportunity to keep the flow attached at minimal input levels, while guarantying that flow separation will be not be allowed to occur. A simple approach was adopted that uses a fast response pressure sensor located near the leading-edge of the airfoil for feedback control. Since a pressure coefficient is required for this purpose, two additional quick responding sensors were installed in the Pitot tube that measures the free stream velocity. The proposed controller used a prescribed pressure coefficient to keep the flow attached. The impact of the time delay on the stability of the controller is briefly discussed and accounted for. The robustness of the controller was demonstrated under varying free stream velocities.

Nomenclature

c	=	chord length
C_L	=	lift coefficient: $L / q\, c$
C_P	=	pressure coefficient: $(p - p_\infty) / q$
C_{pl}	=	C_P maximum threshold value
C_Q	=	steady volume flow coefficient: Q / cU
C_μ	=	steady momentum coefficient: $(2h/c)(U_{Slot}/U)^2$
$<c_\mu>$	=	oscillatory momentum coefficient: $(h/c)(U_{SlotMax}/U)^2$
f	=	frequency of excitation
F^+	=	non-dimensional frequency: $(f\, x_c / U)$
h	=	slot width
i	=	iteration number
L	=	lift
LE	=	leading-edge
q	=	dynamic pressure: $\frac{1}{2}\, \rho U^2$
Q	=	volume flow through the slot
Re	=	Reynolds Number: $U\, c / \nu$

* Research Assistant Professor, AME Dept., The University of Arizona, AIAA Member.
† Graduate Student, AME Dept., The University of Arizona, Student AIAA Member.
‡ Graduate Student, AME Dept., The University of Arizona, Student AIAA Member.
§ Professor, AME Dept., The University of Arizona, AIAA Fellow.
** Research Engineer, Flow Physics & Control Branch, Mail Stop 170, Senior Member AIAA.

RT = Real-Time
t = time
t_d = time delay
TE = trailing-edge
U = free stream velocity
V = control voltage
V_m = voltage margin
V_{max} = maximal voltage
V_s = stationary control voltage
x_{Cp} = the location of the center of pressure

Δt = sampling time
ΔV = voltage decrement
α = angle of attack
θ = angular distance on the TE circular cylinder
τ = pulse width
τ_D = dead time
τ_R = rise time
τ_V = vortex-delay time

I. Introduction

SEPARATED flow over a deflected flap shown schematically in Fig. 1 could be forced to reattach by the introduction of periodic excitation (having no net mass flux) through the slot[1]. This was achieved at a wide spectrum of frequencies provided the amplitude of the perturbations was sufficiently large. It was observed that the most effective dimensionless frequencies requiring the smallest amplitude to force flow reattachment varied between $0.7<F^+<1.5$. On the other hand preventing attached flow from separating could be achieved at substantially lower amplitude provided the frequency was also increased to a higher value of $F^+ > 2$. A very sensitive indicator in this case was the center of pressure, x_{Cp}, that hovered around the mid flap when the flow was separated but moved closer to the leading-edge for attached flow. An example of the movement of x_{Cp} with increased $<c_\mu>$ at a predetermined frequency of $F^+=0.7$ is plotted in Fig. 1. At $<c_\mu>_r = 25*10^{-4}$ the flow reattached and x_{Cp} dropped from 0.45 to approximately 0.2 (arrow two in Fig. 1). Thereafter it was possible to reduce $<c_\mu>$ by an order of magnitude (arrow three) while keeping $x_{Cp}<0.3$ before separation brought it back to 0.5. As long as the flow did not separate (arrow three) one could increase or decrease the amplitude and the result was reversible. By increasing the frequency after reattachment, the value of x_{Cp} remained almost constant along path three. This seems to be a perfect opportunity for closed loop control of separation where one wants to fly under normal post stall conditions but keep the flow attached using fluid control. One wants to achieve that goal at minimum input of momentum and yet be assured that separation will not be allowed to occur.

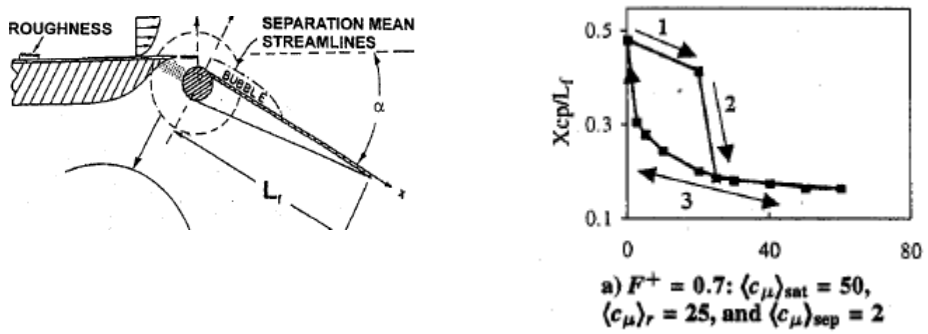

Figure 1. The generic flap and the dependence of x_{Cp} on $<c_\mu>$ at $F^+=0.7$ [1].

It was shown that the transient time of re-separation and re-attachment of the flow on the generic flap[2, 3] and on the GLAS II airfoil[4] scales with the time of flight between the actuator and the trailing-edge when the periodic excitation is applied. This is associated with the amount of fluid that has to be entrained by the vortices created by the actuation and their phase velocity is proportional to the free stream velocity[2, 3]. The basic understanding of underlying physics is necessary for finding proper scaling of the transient time in case when constant suction or blowing replaces periodic actuation. The knowledge of the scaling is most important for practical applications such as closed-loop control under varying speed.

The closed-loop control strategy, described above, is based on the identification of a hysteresis loop by preliminary measurements under the predetermined flow conditions. Such measurements consist of the series of open-loop tests, providing the information about the theshold values of control authority, necessary for keeping the flow attached. Even for one freestream velocity and angle of attack, the amount of work necessary to identify the process precisely, is significant. For the series of free stream velocities and angles of attack, or for the more general case of the flow with varying conditions, such as wind gust, turbulence, etc., representing real flight conditions, the identification part of the control becomes to be enormous. The price of the control fault could be very high, since it may lead to the abrupt drop in lift, increase in drag, etc. This raises the need for more flexible control strategy, which will permit to safely adapt the control algorithm to the changing environment.

Currently very few experimental closed-loop separation control studies have been reported in the literature. Allan et al.[5] modeled the separated flow by a canonical second order system in order to improve the time response of the control system. Banaszuk et al.[6] used an extremum-seeking control algorithm to optimize the pressure recovery in a diffuser. More recently, Tian et al.[7] used nonlinear adaptive control of disturbance rejection to maximize the lift-to-drag ratio of the NACA 0025 airfoil. Pinier et al.[8] implemented the proportional control, based on the POD methodology, to flow separation. Becker et al.[9] used an extremum-seeking algorithm for the separation control. To the best of the authors' knowledge, no attempts to take advantage on the hysteresis through the closed-loop control were published.

All of the above mentioned closed-loop approaches achieved the control over the time scale which is much larger than that of the flow dynamics. The possible reason for that is the time delay between the control surge and the flow reaction, which could lower the anticipated performance of the control algorithms, or even render them unstable.

The current approach is based on the simplistic closed-loop control of classical predictive logic, which uses the preliminary hysteresis measurements and apply them to the flow with fixed freestream conditions. The purpose of the investigation is to validate and broaden the concept of using the hysteresis for closed-loop control by applying it to an airfoil and to other modes of fluidic control, such as constant suction that is described below.

II. Experimental Apparatus and Procedures

The elliptical airfoil used in the present experiment has a chord of 10.86" and a maximum thickness of 30% chord. The circular arcs that form its leading and trailing-edges are 2.46" in diameter and they fit snuggly into the main body of the airfoil. The slots are inclined at 30^o to the tangent and their width and location can be adjusted in situ by rotating the individual arcs and placing the appropriate shim stock into the slots before tightening the end plates. The symmetry of the configuration enables tests at positive and negative incidence angles thus changing the orientation of the slot relative to the oncoming stream as well as the surface from which AFC emanates. This might be very important near the leading-edge where acceleration of the flow away from the stagnation point (that is generally located on the lower surface) might affect the stall angle and the behavior of the airfoil near stall.

One may obtain data by either placing the minor or the major axis of the ellipse normal to the flow. The major axis always represents the chord while the minor one represents the maximum thickness of the elliptical airfoil. Under normal flight conditions the major axis is inclined slightly to the oncoming flow. However but by rotating the ellipse at 90^o to the flow, the airfoil simulates the two dimensional equivalent of a tiltrotor wing in hover, thus measuring its download. Fig. 2 shows the slots as aligned in the current experiment with the flow coming from the left. Suction is applied to the LE cylinder. An "I" beam divides the interior volume of the airfoil into two independent pressure chambers through which blowing, suction or ZMFF can be passed either independently or in conjunction with one another.

The airfoil is equipped with 60 static pressure taps (Fig. 2) from which lift and form drag were calculated. Total drag was measured by traversing the wake some 3 chord lengths downstream of the trailing-edge where the static pressure corrections were small. The rake consists of 19 total-pressure probes that were placed at an interval of 1" and two static pressure probes located at both ends of the rake. The

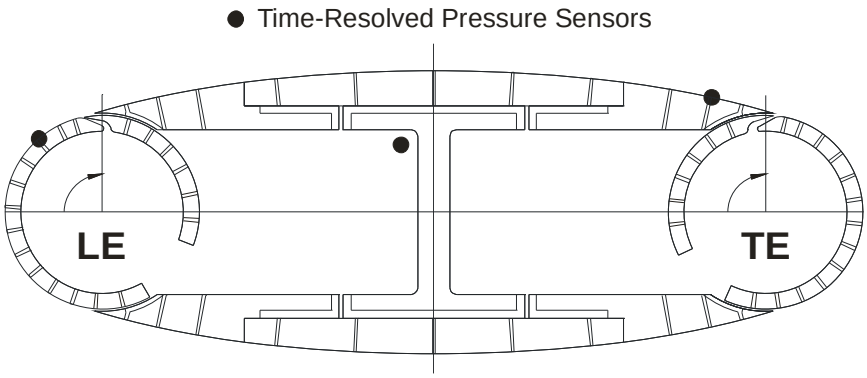

Figure 2. The elliptical airfoil.

rake could slide relative to the airfoil and could be centered in the wake. It could also be traversed across the wake in order to provide the necessary resolution of data points wherever the velocity gradients were steep. All the pressure ports were scanned electronically using a PRESSURE SYSTEMS INC. (PSI) model 780 equipped with six 16-port differential pressure scanners. These scanners have an array of silicon piezo-resistive pressure sensors, one for each pressure port. The sensors are calibrated by connecting them all to a common manifold of known pressure. All the sensors are calibrated by exposing them to a prescribed identical pressure through two-position pneumatically actuated valves.

The 24" span model was installed in a 24-inch by 41-inch test section of an open-loop, cascade wind tunnel. The Reynolds number tested varied between 100,000 and 500,000. In order to avoid laminar bubbles and strong Reynolds number dependence, four roughness strips were used, two were placed at mid chord (x/c=0.52) and two at the juncture between the LE cylinder and the main element (x/c=0.12)[*]. The installation of the airfoil in the tunnel is shown in Fig. 3.

For the open-loop part of the experiment a single centrifugal blower was used for sucking the air through the slot. This blower could provide up to 68 SCFM at a maximum pressure of 35 inches of water.

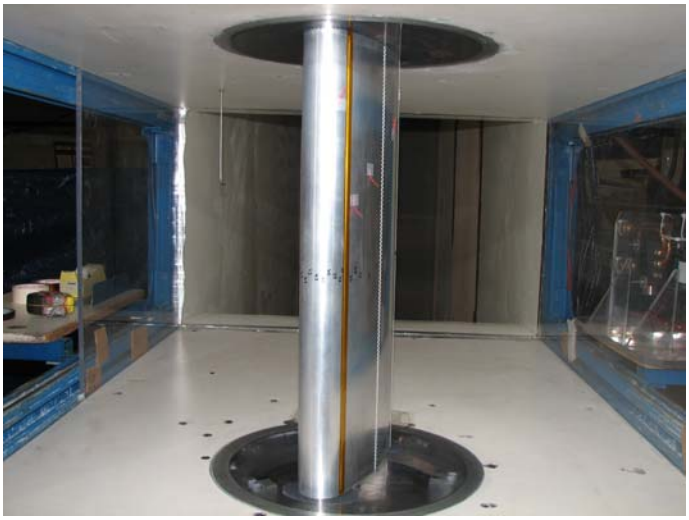

Figure 3. A picture of the airfoil in the wind tunnel.

[*] The current tripping is different from that, described in Ref.[10].

The air leaving the settling chamber in the interior of the airfoil passed through two equal flexible hoses that were connected to each side of the settling chamber.

The flow rate could be regulated by changing the RPM of the blower and it was monitored by using an appropriate flow meter.

For the closed-loop control two Venturi pumps (VACCON model VDF 750), that were connected to both sides of the airfoil's interior chamber, provided the required suction, see Fig. 4. High pressure air (100 psi) was supplied to these pumps through the proportionally controlled valve, that was regulated by a controller.

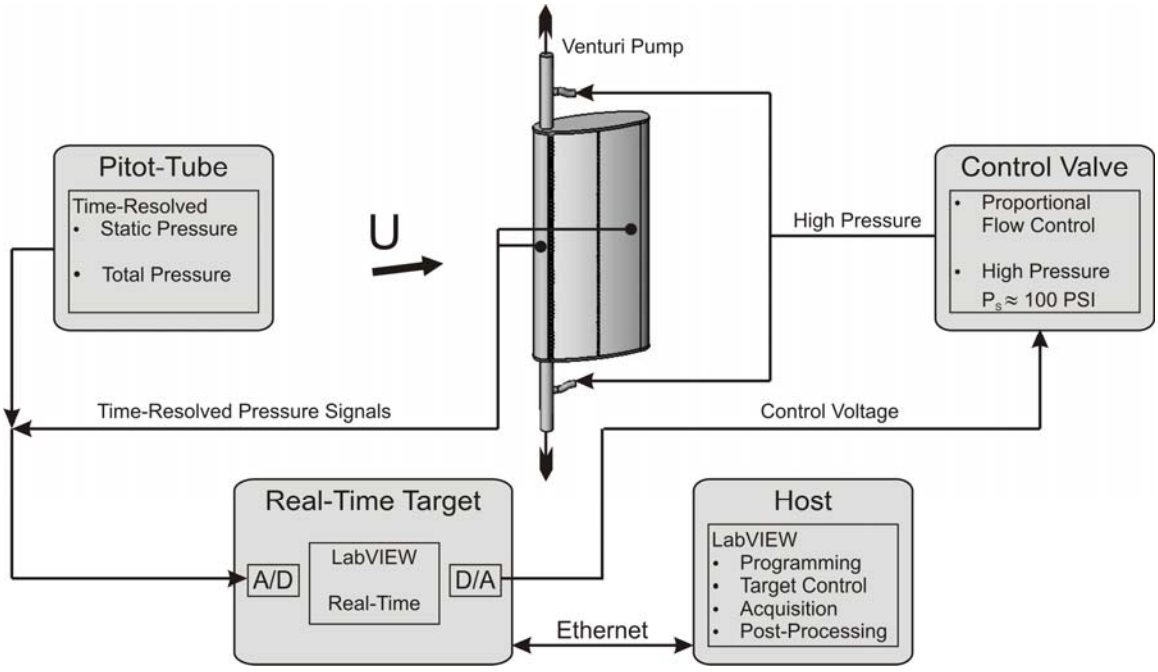

Figure 4. Sketch of the closed-loop system.

LabVIEW REAL-TIME (RT) module was used for the development and implementation of the closed-loop algorithm. The RT operational system (LabVIEW ETS) guarantees an exact timing and determinism of the algorithm processes. The RT target used was a NATIONAL INSTRUMENT (NI) PXI-1011, with a NI 8175 controller, equipped with INTEL PENTIUM III 866MHz CPU. The host computer is a standard PC that runs LabVIEW REAL-TIME and communicates with the RT target through the Ethernet. The control loop frequency was 1 kHz, and the worst-case time jitter was 60μs.

Four dynamic pressure sensors (ENDEVCO model 85701C-1) were used for feeding back the controller. Two of the sensors were connected to the taps of the airfoil: one upstream the slot (x/c=0.05) and another close to the trailing-edge (x/c=0.82), see Fig. 2. Two other sensors were connected to the Pitot tube of the wind tunnel, permitting real time normalization of the pressures converting them to C_Ps. It is well-known that the C_P values at the attached/separated flow states at different free stream velocities and at the same incidence are almost equal. This fact is exploited in the closed-loop part of the experiment, in which the admissible C_P thresholds are specified rather than not normalized pressure ones.

One additional pressure sensor (SILICON MICROSTRUCTURE model SM5652-015) was installed inside the airfoil chamber for monitoring the suction. All pressure sensors were connected through the SCXI 1520 unit to the target computer. The pressure signals were low-pass filtered at 10kHz. A NI PXI 6052E board fed the control signal to the valve controller.

For the current experiment the slot was fixed at 90° from the LE in a clockwise direction relative to the chord. It pointed upstream and its width was h=0.015".

III. Open-Loop Control Results

The C_L-α plot is shown in Fig. 5, where it becomes obvious that the elliptical cylinder behaves very much like a thick symmetrical airfoil (strut). Separation progresses from the trailing-edge upstream and that progression starts already at α=6° at the Reynolds number shown (Re=2.3*10^5). Maximum lift, C_{Lmax}=1.1, is obtained at α=16°. Applying steady suction of C_μ =1.7% delays the stall angle by more than 10° and increase C_{Lmax} to 2.1. Due to the bluff trailing-edge the (L/D) of this airfoil is of the order of 10 and suction increases it by 100%. The variation of C_D with α is also plotted in Fig. 5. The details of corresponding pressure distributions are shown in Fig. 6.

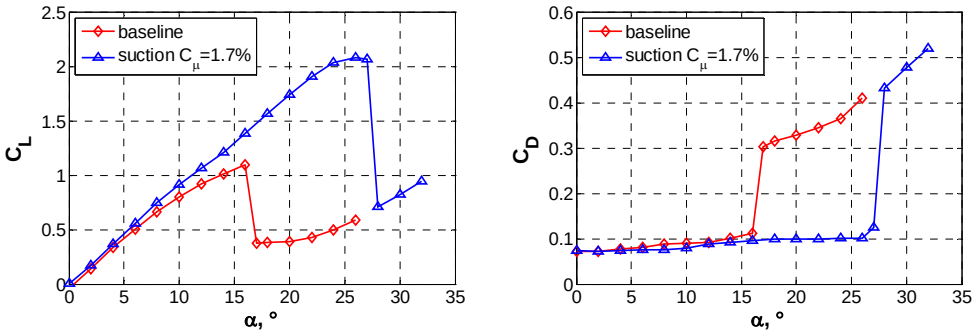

Figure 5. Lift and drag generated by the elliptical airfoil at U=15m/s, α=19°.

The question arises how a stalled airfoil, at α=19° say, recovers from its stall after a steady suction is applied on its upper surface near the leading-edge. At very low suction levels, see Fig. 7, the flow does not reattach and the drag remains almost constant since the removal of fluid possessing low axial momentum is insignificant (sink drag). Concomitantly the lift stays almost at the same level. When the sucked momentum coefficient exceeds 1.7% the flow reattaches to the upper surface resulting in a remarkable decrease in drag (from C_D=0.33 to C_D=0.11) and a four-fold increase in lift. One may then reduce the suction level from the previous C_μ=1.7% to approximately 0.2% before any noticeable change in the lift or drag occurred. The implication is that it takes about eight times larger C_μ to attach separated flow than to

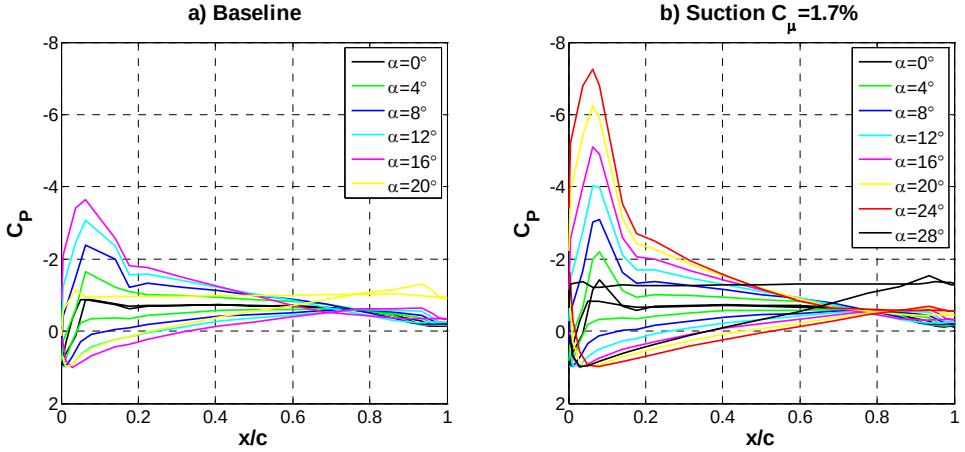

Figure 6. C_p distributions along the airfoil, U=15m/s, α=19°. a) baseline, b) suction C_μ =1.7%.

maintain attached flow under otherwise identical conditions. One hopes that by continuously monitoring the flow and controlling the suction parameters one could maintain attached flow conditions at the lowest possible level of intervention and do so safely.

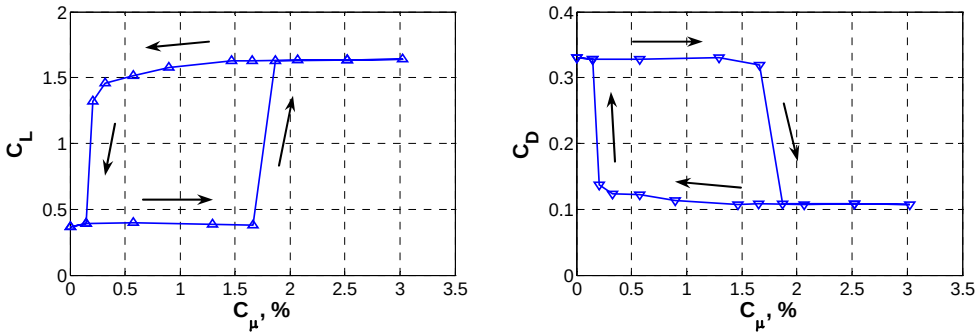

Figure 7. The hysteresis created by suction at U=15m/s, α=19°.

Examining the pressure distributions at identical levels of C_μ=0.14-1.50% revealed that the absolute value of the pressure coefficient near the leading-edge of the ellipse dropped from -6 to -0.9 when LE separation occurred (Fig. 8). This fact is used in the currently adopted approach to the closed-loop control of the hysteresis, where only the leading-edge sensor is employed for deciding what control voltage should be applied to the valve.

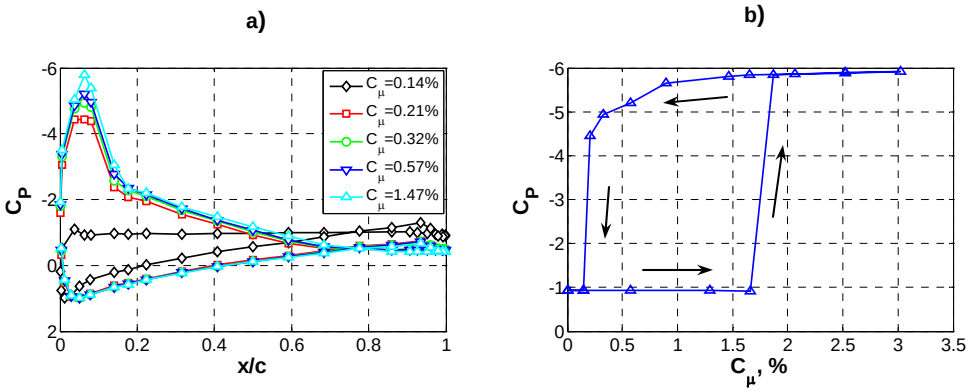

Figure 8. Pressure distributions at U=15m/s, α=19° at different levels of suction. a) over the airfoil, b) at x/c=0.06.

Another indication of the difference between the attached and separated flow conditions is the wake. Wake surveys were made and the two wake profiles corresponding to the extreme pressure distributions are

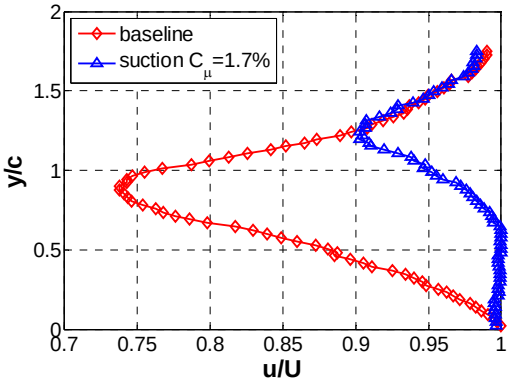

Figure 9. Two velocity distributions in the wake of the airfoil at U=15m/s, α=19°.

plotted in Fig. 9. One curve corresponds to the separated flow and the other to the attached one at identical incidence. Not only the velocity deficit is much larger in the separated flow case but the mean location of the wake center line differs by as much as 0.3c. Using this fact for a closed-loop sensor is much more difficult to implement experimentally.

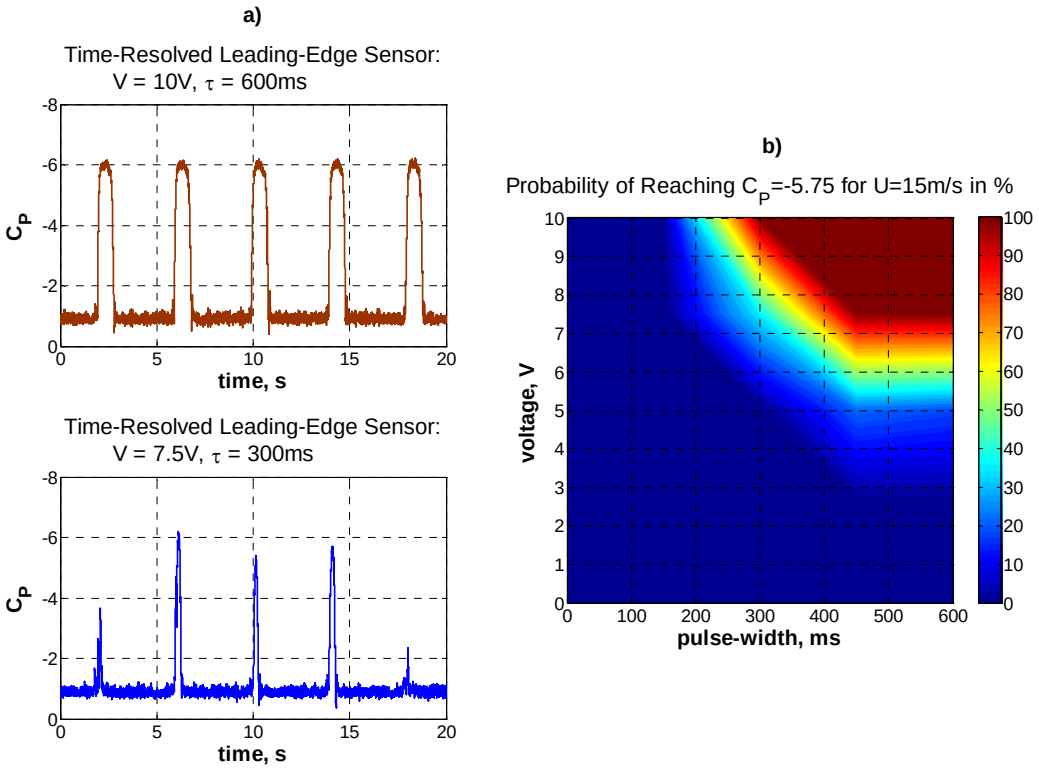

Figure 10. Probability chart of the reattachment from complete separation by applying the pulses with different amplitudes and time widths at U=15m/s, α=19°.

A series of the experiments, examining the dynamics of reattachments that are followed by separations were conducted by applying periodic control voltage pulses of different durations and amplitudes to the high-pressure valve, inducing the suction through the slot. Depending on the relation between the pulse width and its amplitude the flow is attached, separated, or partly attached as could be seen from Fig. 10a. Hundred pulses were generated and recorded to estimate the probability of reaching the prescribed C_P value, and the result is shown in Fig. 10b. Not suprising, the flow attaches for the time-voltage values, corrresponding to the right upper coner of Fig. 10b.

For the combinations of pulse amplitude and width, that resulted in a complete reattachment of the flow with 100%-probability, C_P of the leading and trailing-edge sensors as well as the pressure in the interior of the airfoil were phase-locked to the input signal and were ensemble-averaged. The results are shown in Fig. 11 for different free stream velocities.

The different time scales, such as dead time, τ_D, i.e. the time delay required for the pressure to drop at the leading-edge sensor, the vortex-delay time, τ_V, that corresponds to the time delay required for the trailing-edge sensor to record its first transient increase in pressure and rise time, τ_R, that is represented by the steepest slope that would have reached a steady state pressure. All three time-scales are clearly seen in Fig. 11a where they are also defined. The constant suction applied at τ=0 lowered the pressure in the interior chamber by a given increment and the time required to achieve this was constant independent of the free stream velocity. The transient evacuation of the interior air by suction is likely to depend on the chamber volume and it requires some 200ms in the present case. On the other hand, the rise times and the dead times sensed near the leading-edge, depend on the free stream velocity but this dependence is not

simple because both C_Q and C_μ for a prescribed voltage input depend on the free stream velocity. Once a threshold in either of these coefficients is exceeded the C_P near the leading-edge starts to drop and it therefore depends on U. For the closed-loop applications, diminishing the dead time is important for the stability of the control. Since the leading-edge cylinder is open to the rest of the airfoil interior, it would be interesting to limit the volume of the suction chamber and observe its effect.

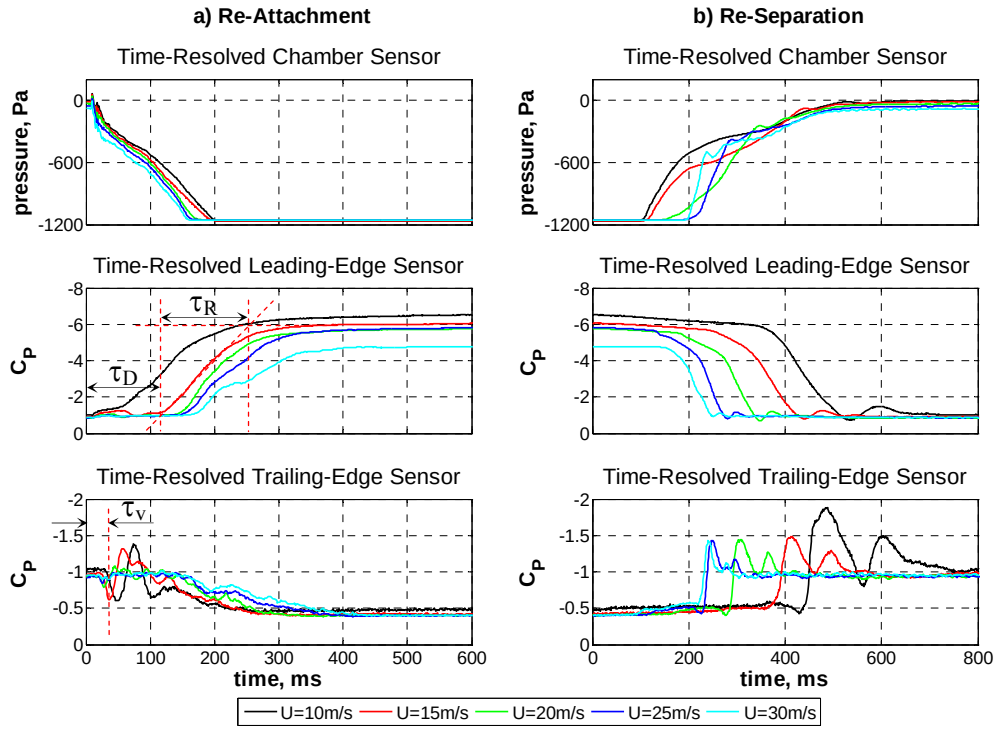

Figure 11. Time-resolved phase averaged pressure signatures at α=19° under pulse voltage 10V and pulse width 600ms.

The striking feature of the pressure signature at the trailing-edge sensor is the presence of substantial oscillations at the beginning of the reattachment and the separation processes, see Fig. 11b. Similar observations were made by Darabi[2, 3], however in this case the separation process may be involved with the creation of the dynamic stall vortex.

IV. Closed-Loop Results

The following preliminary experiment was performed to clarify the influence of the time delay on the controller performance. Initially the flow, normally separated at U=15m/s, α=19°, was attached by suction at the maximum available control voltage, 10V. Then the voltage was decreased in steps of 0.1V-per step lasting from 10 to 200ms, for three sets of the experiments (Fig. 12). For each experiment the pressure was continuously monitored and the C_P coefficient was calculated at every step. If C_P exceeded the threshold value -4.5 (i.e. the suction on the upper surface near the LE decreased to -4.5), the controller immediately generated the maximum available voltage, eventually attaching completely the flow and the whole process would be repeated. The C_P drop overshot this value for all cases, however it was bigger for the shorter step durations, resulting in more complete separation in the case with 10ms. To understand this result the delay of the flow relative to the control voltage should be accounted for. If the controller "waits" long enough for the reaction of the flow so that it becomes comparable with the time delay, the C_P drop overshoot is

minimal, otherwise the control is unstable. Note that the voltage dropped way below the value of 4 in Figure 12c and the C_P detected by the LE sensor to -1, thus a proper relation between the minimum voltage and the ensuing C_P should be satisfied.

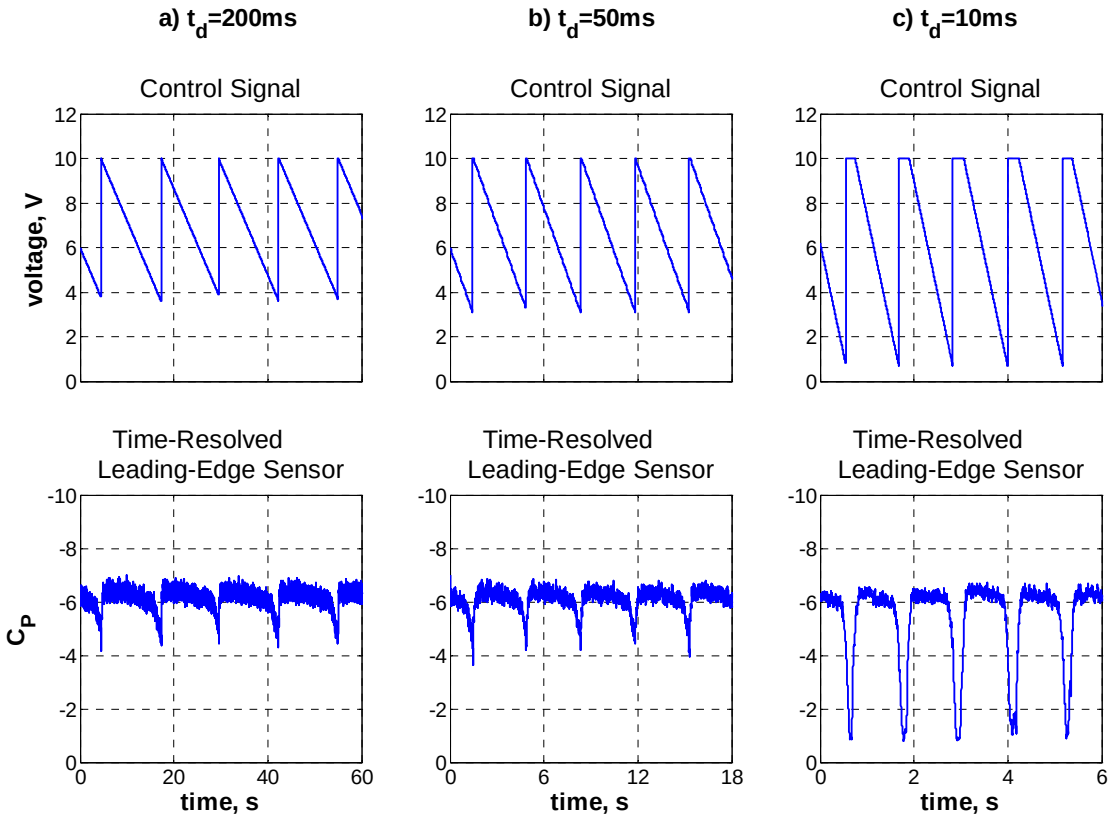

Figure 12. The duration time effect on the controller ability to keep the flow attached, U=15m/s, α=19°, C_P-threshold =-4.5.

Consider the operation of the closed-loop control. Before it begins, the flow is forced to reattach by increasing C_μ corresponding to the lower branch of the C_L-C_μ curve shown in Fig. 6. The time history of the applied voltage and the ensuing C_P coefficient are shown in Fig. 13a. The voltage, applied to the valve, is increased by steps of 0.1V unless the prescribed value of C_P =-2 is attained. It was experimentally found that once this threshold C_P value is exceeded, the flow will eventually reattach. Each applied voltage level lasted 200ms to account the delay between the applied control and the flow reaction. Notice the typical presence of several sharp pressure pulses which are the precursors of complete reattachment. If after such oscillations the pressure returns to its initial level for a while, the voltage continues to increase until reattachment is complete.

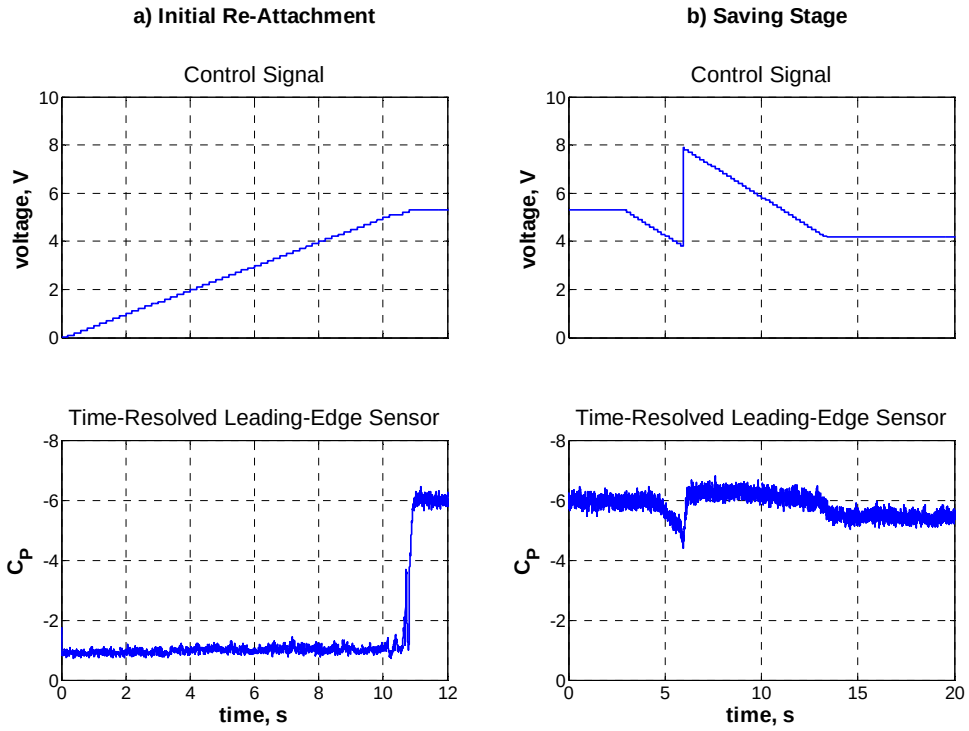

Figure 13. U=15m/s, α=19°. a) Time history of the reattachment, b) the closed-loop saving mode.

A simple approach for the closed-loop algorithm was adopted at present, and the block-diagram of the algorithm is shown in Fig. 14. It is based on finding the correspondence between the voltage applied to the valve and the resulting real-time C_P values observed along the hysteresis loop, that provide information about the theshold value required to maintain control authority necessary for keeping the flow attached. The first stage of the closed-loop algorithm is the identification of the minimal voltage that corresponds to the maximum permitted value of C_P defined by the user. This is implemented by gradual stepwise decrease of the voltage until the threshold C_P value is achieved. For every voltage step the waiting interval is comensurate with the transient time lest the premature low voltage level would cause separation. This is acomplished through the instructions 1 and 2 of the controller (Fig. 14), according to which unless the time counter t_i is smaller than the time delay t_d the voltage level will remain at its current level, awaiting the reaction of the flow. If at some instance C_P becomes bigger than C_{pl}, the control voltage *immediately* increases to the prescribed maximum value, V_{max} , (see the instruction 3 of the controller). V_{max} is chosen in advance to assure that the flow will not separate. If $C_{p\,i-1}>C_{pl}$ occurs for the first time (i.e. $C_{p\,i-2}<C_{pl}$) then the corresponding voltage, V_{i-1} , is the critical voltage under the existing conditions and the stationary voltage value is updated to $V_{si} = V_{i-1}+V_m$, where V_m provides a safety margin, taken as being 10% of V_{i-1} in this experiment. If the occurrence of $C_{p\,i-1}>C_{pl}$ returns (i.e. $C_{p\,i-2}<C_{pl}$), the stationary voltage remains the same as in the previously sampled step. After several time steps the increase of voltage takes effect on the flow and $C_{p\,i-1}$ becomes smaller than C_{pl}. At this stage the controller follows instructions 1 and 2, and reduces the voltage slowly until the stationary voltage V_s is achieved. According to the previous identification stage this voltage is larger than the voltage, at which $C_{p\,i-1}>C_{pl}$ occurred, consequently, if the flow conditions do not change, the flow should remain attached at that control level. This closed-loop operation corresponds to the saving stage of the flow control as shown in Fig. 13b).

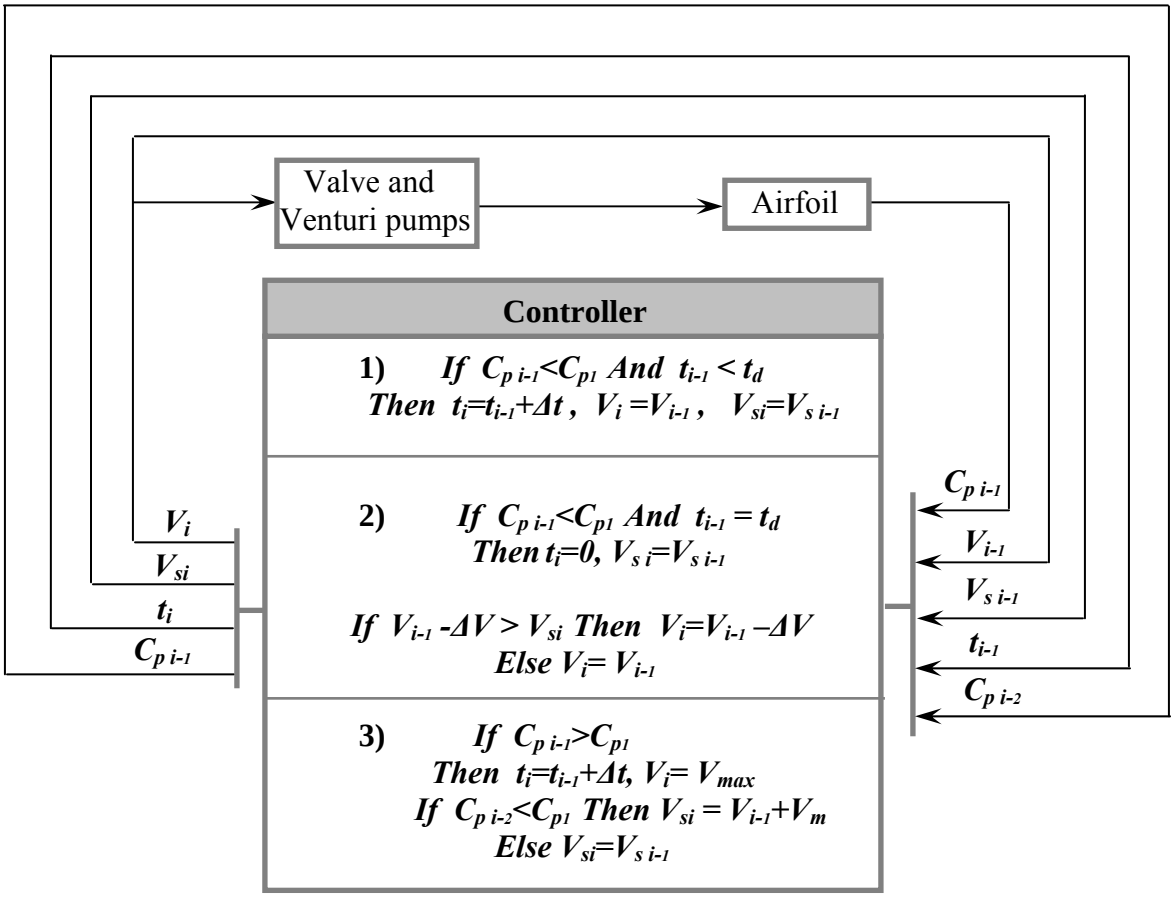

Figure 14. Block-scheme of the closed-loop control.

To examine the robustness of the controller under consideration the wind tunnel speed was increased from 15m/s and 20m/s, thus reducing the C_Q (or C_μ) of the suction that was maintained at a prescribed voltage level (Fig. 15). The wind tunnel inertia resulted in a relatively long transient velocity time of approximately 5s. Performance of the open-loop and the closed-loop controls were compared. Whereas the open-loop control failed to keep the flow attached, the closed-loop performed well. In some cases several control cycles such as that, shown in Fig. 15b are necessary for stabilization the flow state.

Similar logic could be easily implemented for limiting C_P from the bottom in the case of diminishing velocity.

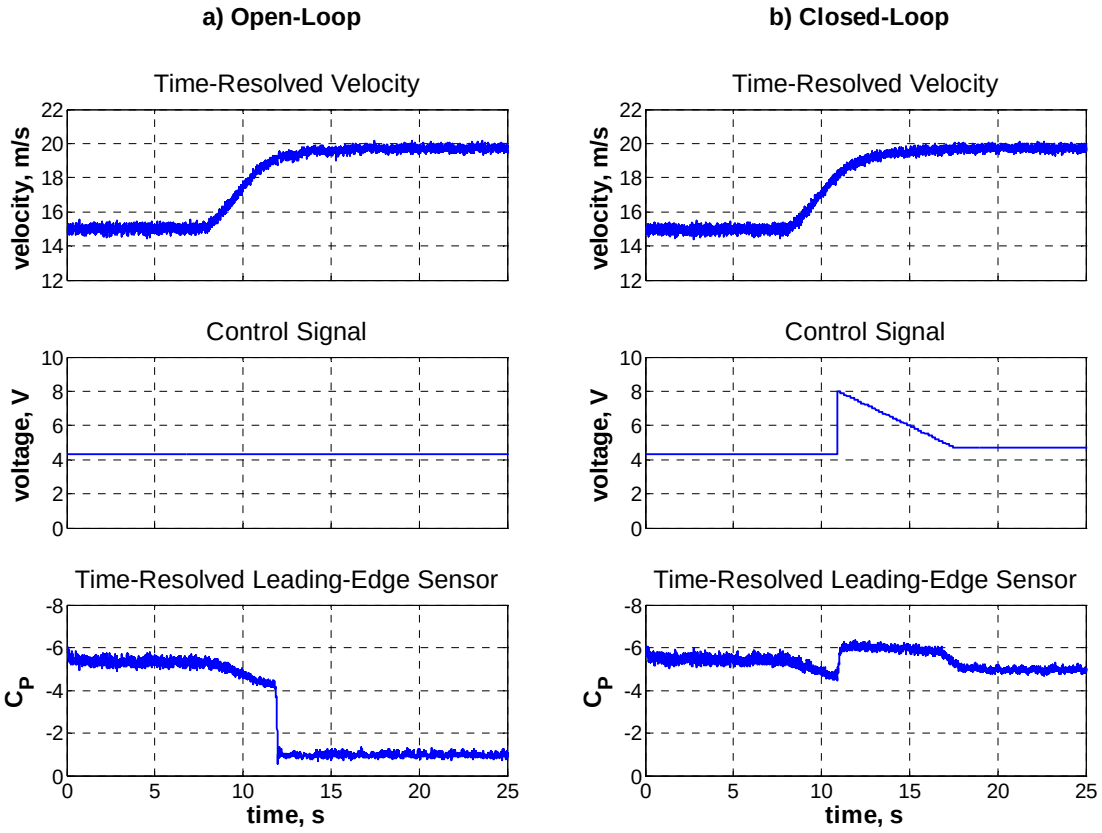

Figure 15. Testing the robustness of the controller to changes in the free stream velocity: a) open-loop, b) closed-loop control.

V. Conclusions and Suggestions for Further Research

Different levels of suction are required to force a separated flow over an elliptical airfoil to reattach than to prevent an attached flow from separating under normally stalled conditions. This is just one example of hysteresis that could occur under different flow conditions and flow control strategies. Such strategies could include, but would not be limited to constant blowing or periodic excitation. The concept of the hysteresis feedback control was proposed and developed, permitting to keep the flow safely attached at the lowest possible input of energy.

Preliminary open-loop experiments show that attaching the flow by pulsing suction requires a specific relationship between the pulse amplitude and its duration that defines the probability of reattachment. Different time scales of the reattachment, such as dead time, vortex-delay time and rise time, were defined for the specific configuration used.

It was found that when C_μ is reduced within the limits that keep the flow attached, the C_P measured near the leading-edge is being significantly modified, while the the C_P measured near the TE remains almost unaffected. This fact is used in the closed-loop control strategy where only the leading-edge sensor was employed by the feed-back controller. To eliminate the sensitivity to the free stream velocity variations in C_P have been used rather than the raw pressure readings for defining the feedback threshold. The impact of the time delay on the closed-loop control stability was discussed and demonstrated experimentally and some simple accounting of the delay was implemented in the controller. The robustness of the closed-loop control was demonstrated by varying wind tunnel velocity, where the open-loop failed to keep the flow attached, while the closed-loop succeeded to do so.

The current investigation should be expanded to include:

1) C_L and consequently, C_P values of the attached flow are significantly modified when the angle of attack changes as does the size of the hysteresis loop (Fig. 16). For this reason the current technique should be expanded to accept various threshold levels and be amenable to changing flow angles as well as speeds. A simple alternative could be based on a temporal derivative of C_P whose threshold exceeds a prescribed value. This might be a more practical approach to turbulence alleviation that has to cope with simultaneous changes in speed and in incidence.

2) Predictive control, based on the system identification technique, as described in Ref.[7] could be tried in hysteresis feedback control. In the framework of the approach an apriori knowledge of flow dynamics is unnecessary when system identification is used.

3) Additional direction for the development of the adaptive control could be based on the properties of the hysteresis, which should be carefully studied and documented. The non-stationary signatures of the pressure sensors and their phase-averaged transients may be of significant interest. The sensitivity of the hysteresis thresholds to these perturbations could provide the information about admissible control authority margins.

4) The expansion of the current approach to other types of flow control, such as steady blowing, periodic excitation or the use of sweeping jets could be of interest.

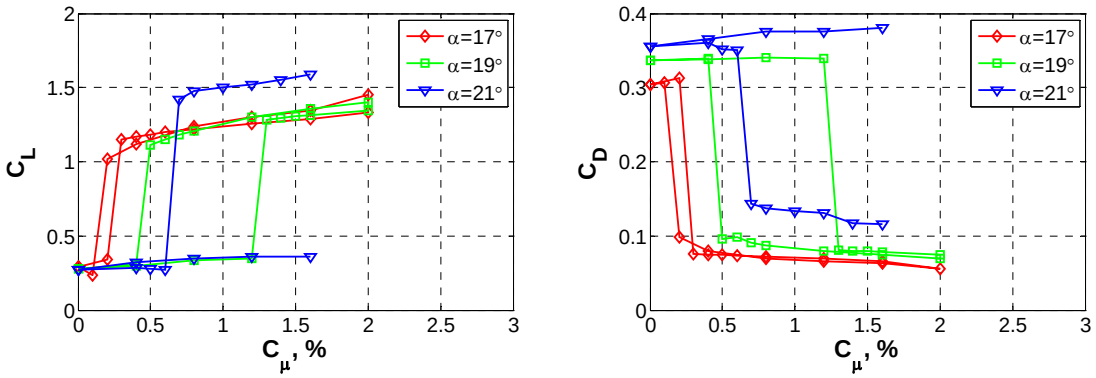

Figure 16. CFD results [11] for suction hysteresis at *U*=15m/s.

Acknowledgment

The authors are grateful to Lutz Taubert for his help in preparation the experiment. The work was partially supported by a NASA NRA under grant No: NNX07AB73A#1.

References

[1]Nishri B., and Wygnanski I., "Effects of Periodic Excitation on Turbulent Flow Separation from a Flap", *AIAA J.*, Vol. 36, No. 4, 1998, pp. 547-556.

[2]Darabi, A., and Wygnanski, I., "Active Management of Naturally Separated Flow Over a Solid Surface. Part 1. The Forced Reattachment Process", *J. Fluid Mech.,* 2004, Vol. 510, pp. 105–129.

[3]Darabi, A., and Wygnanski, I., "Active Management of Naturally Separated Flow Over a Solid Surface. Part 2. The Separation Process", *J. Fluid Mech.,* 2004, Vol. 510, pp. 131–144.

[4]Zakharin, B., and Wygnanski, I., "On the Mechanisms of Forced Separation and Reattachment of Flow to a Modified GLAS II Airfoil", accepted to *J. of Aircraft*.

[5]Allan, B., Juang, J., Seifert A., Pack L. and Brown, D, "Closed-loop Separation Control Using Oscillatory Flow," *ICASE Report* No. 2000-32, 2000.

[6]Banaszuk, A., Narayanan S., and Zhang Y., "Adaptive Control of Flow Separation in a Planar Diffuser," *AIAA Paper* 2003-0617, Jan. 2003.

[7] Tian, Y., Cattafesta, L., and Mittal R, "Adaptive Control of Separated Flow," *AIAA Paper* 2006-1401, Jan. 2006.

[8] Pinier, J.T., Ausseur, J.M., Glauser, M. N., and Higuchi H., "Proportional Closed-Loop Feedback Control of Flow Separation", *AIAA J.*, Vol. 45, No. 1, Jan. 2007.

[9]Becker, R., King, R., Petz, R., and Nitsche, W., "Adaptive Closed-Loop Separation Control on a High-Lift Configuration Using Extremum Seeking", *AIAA J.*, Vol. 45, No. 6, June 2007.

[10]Chen, C., Zakharin, B., and Wygnanski, I.J., "On the Parameters Governing Fluidic Control of Separation and Circulation", 46th AIAA Aerospace Sciences Meeting and Exhibit, 7 - 10 January 2008, Reno, Nevada, *AIAA Paper 2008-629*.

[11]Bhamburkar, C., Private Communication.